THEORETICAL CHEMISTRY INSTITUTE

THE UNIVERSITY OF WISCONSIN

MOLECULAR COLLISIONS. XV. CLASSICAL LIMIT OF THE GENERALIZED PHASE SHIFT TREATMENT OF ROTATIONAL EXCITATION: ATOM-RIGID ROTOR

M. D. Pattengill, C. F. Curtiss and R. B. Bernstein

WIS-TCI-436

16 April 1971

MADISON, WISCONSIN

MOLECULAR COLLISIONS. XV. CLASSICAL LIMIT OF THE GENERALIZED PHASE SHIFT TREATMENT OF ROTATIONAL EXCITATION: ATOM-RIGID ROTOR *

by

M. D. Pattengill, C. F. Curtiss and R. B. Bernstein
Theoretical Chemistry Institute and Chemistry Department
University of Wisconsin, Madison, Wisconsin 53706

ABSTRACT

The generalized phase shift (GPS) approach to the problem of rotationally inelastic molecular collisions is extended from the level of the first-order (semiclassical) approximation of paper XIV to the essentially infinite order level, but specialized to the full classical limit. The limitations and assumptions are that 1) the de Boer reduced wavelength parameter be small (i.e., $\Lambda^* << 1$), 2) the relative translational motion takes place under the influence of the orientation-averaged (spherical) part of the anisotropic interaction potential (i.e., curved but planar trajectories), and 3) the rotational energy, E_{rot}, may be well-approximated by its classical expression (i.e., rota-

---

* This research was supported by Grants GP-12832 and GB-16665 from the National Science Foundation and Grant NGL 50-002-001 from the National Aeronautics and Space Administration.

tional quantum numbers $>> 1$). The procedure is applied numerically to a model problem involving an anisotropic L.-J. (12,6) potential (as in XIV), taking advantage of the previously computed generalized action integrals. The program yields directly an arbitrarily chosen specified number of moments of the inelasticity probability density function $\mathcal{P}(\Delta E_{rot})$ at various impact parameters b . Inversion of the set of moments leads to $\mathcal{P}(\Delta E_{rot})$. For the examples chosen, the lowest eight moments sufficed to obtain practical accuracy of convergence on the inversion. For large b , i.e., in the weak-coupling regime, the first moment vanishes and the second moment (which can be well-approximated using the first-order results of XIV) dominates, governing the breadth of the inelasticity density function.

In paper XIV of this series,[1] the lowest (first-order) approximation of the generalized phase shift[2] (GPS) treatment of rotationally inelastic molecular collisions was applied to the case of atom-rigid rotor scattering. While restricted to "high" initial rotor energies,[3] these calculations were of a semiclassical nature (i.e., classical relative translational motion but quantized rotor energy levels). The present work takes advantage of the recent development[4] of a method of implementation of the "infinite-order"[5] approximation of the GPS method, applied to systems of the type considered in XIV. The present calculations are limited to the purely classical regime. As is discussed below, this restriction permits the use of a relatively simple procedure for obtaining the moments of the rotational inelasticity probability density function. Inversion of a set of the moments then yields the density function itself.

In the following, expressions for the moments of the density function are exhibited. These equations are then put into a computationally convenient form, and a method of inverting the moments is described. Finally, numerical results obtained for model systems similar to those considered in paper XIV are presented.

I. MOMENTS OF THE PROBABILITY DENSITY FUNCTION

A series of papers[4] on the transport properties of a gas of diatomic molecules has considered the evaluation of certain sums and integrals of the rotationally inelastic cross sections. In paper II of that series, an expression[6] (Eq. (T.II.27)) was obtained, which, for the case

of atom-rigid rotor scattering, reduces to:

$$\sum_{\ell} (\Delta\epsilon)^{\nu} I(\bar{\ell};\ell;\chi) = \frac{1}{8\pi^2} \int K^{\nu}(L_a L;S) I(L_a;\chi;S)\, dS. \qquad (1)$$

Here, $\bar{\ell}$ and ℓ are respectively the initial and final rotor energy quantum numbers, $\Delta\epsilon$ is the rotational energy change (in units of kT), ν is a non-negative integer, $I(\bar{\ell};\ell;\chi)$ is the degeneracy-averaged differential cross section for scattering at an angle χ, $L_a \equiv \hbar\bar{\ell}$, $L \equiv \hbar\bar{\lambda}$ where $\bar{\lambda}$ indexes the initial relative (orbital) angular momentum, and S is the three dimensional rotation group defined by Euler angles α, β and γ. $I(L_a;\chi;S)$ is given by Eq. (T.II.25), and may be written:

$$I(L_a;\chi;S) = \sum_i \frac{2\pi b_i}{\sin\chi} \left|\frac{\partial b_i}{\partial\chi}\right| \qquad (2)$$

where b_i is the classical impact parameter, and the sum is over the branches of the deflection angle function contributing to a given scattering angle. The quantity $K(L_a L;S)$ is given by Eq. (T.I.56), and, for atom-rigid rotor scattering is:

$$K(L_a L;S) = \frac{2\hbar^2}{I kT}\left\{\left(\frac{\partial H}{\partial\beta}\right)^2 + \frac{1}{\sin^2\beta}\left(\frac{\partial H}{\partial\alpha}\right)^2 - 2\frac{\cos\beta}{\sin^2\beta}\left(\frac{\partial H}{\partial\alpha}\right)\left(\frac{\partial H}{\partial\gamma}\right)\right.$$
$$- (1-\cot^2\beta)\left(\frac{\partial H}{\partial\gamma}\right)^2 - \left[\bar{\ell}^2 - 4\left(\frac{\partial H}{\partial\gamma}\right)^2\right]^{1/2} \qquad (3)$$
$$\left.\times\left[\cos\gamma\left(\frac{\partial H}{\partial\beta}\right) + \frac{\sin\gamma}{\sin\beta}\left(\frac{\partial H}{\partial\alpha}\right) - \cot\beta\sin\gamma\left(\frac{\partial H}{\partial\gamma}\right)\right]\right\}.$$

Here, I is the moment of inertia of the rotor, and H is defined by Eq. (T.I.31):

$$\mathcal{S}(\bar{\ell}\bar{\lambda};S) = \exp\left[2i\,H(\bar{\ell}\bar{\lambda};S)\right] \tag{4}$$

in terms of the quantity $\mathcal{S}(\bar{\ell}\bar{\lambda};S)$. The present results are based on the approximation for $\mathcal{S}(\bar{\ell}\bar{\lambda};S)$ given by Eq. (XII.72). It should be noted that the integration in Eq. (1) is not over the entire rotation group S , but is restricted (cf. Eqs. (T.I.56) - (T.I.62)) to regions in which

$$\left|\left(\frac{\partial H}{\partial \alpha}\right)\right| < \bar{\lambda}/2 \tag{5}$$

and

$$\left|\left(\frac{\partial H}{\partial \gamma}\right)\right| < \bar{\ell}/2. \tag{6}$$

With Eqs. (2) and (3), Eq. (1) may be transformed to yield:

$$\sum_{\ell} (\Delta\epsilon)^{\nu} P(\bar{\ell};\ell;\bar{\lambda}) = \frac{1}{8\pi^2}\int K^{\nu}(L_a L;S)\, dS \tag{7}$$

where $P(\bar{\ell};\ell;\bar{\lambda})$ is the probability of transition from rotor state $\bar{\ell}$ to ℓ at an initial relative angular momentum indexed by $\bar{\lambda}$. Eq. (3) for $K(L_a L;S)$ gives the classical limit. Thus, the sum on the $/hs$ of Eq. (7) should be replaced by an integral, yielding:

$$\int (\Delta\epsilon)^{\nu} P(\bar{\ell};\ell;\bar{\lambda})\, d\ell = \frac{1}{8\pi^2}\int K^{\nu}(L_a L;S)\, dS \tag{8}$$

where $P(\bar{\ell}; \ell; \bar{n})$ is now a continuous distribution in the quantum number spaces. It is more convenient to transform to the corresponding energy spaces through the classical relation:

$$\epsilon(\ell) = \frac{\ell^2 \hbar^2}{2 I k T} . \tag{9}$$

Thus we define

$$\tilde{P}(\bar{\epsilon}, \Delta\epsilon, b) \frac{\partial \epsilon}{\partial \ell} = P(\bar{\ell}; \ell; \bar{n}) \tag{10}$$

so that Eq. (8) becomes

$$\int (\Delta\epsilon)^\nu \tilde{P}(\bar{\epsilon}, \Delta\epsilon, b) d\epsilon = \frac{1}{8\pi^2} \int K^\nu(L_a L; S) dS. \tag{11}$$

or, in terms of the change, $\Delta\epsilon$,

$$\int (\Delta\epsilon)^\nu \tilde{P}(\bar{\epsilon}, \Delta\epsilon, b) d(\Delta\epsilon) = \frac{1}{8\pi^2} \int K^\nu(L_a L; S) dS. \tag{12}$$

Eq. (12) thus gives the moments of the rotational inelasticity probability density function in terms of three dimensional integrals of powers of the quantity $K(L_a L; S)$.

II. MODEL CALCULATIONS

A. Methodology

As for the model calculations of paper XIV, the atom-rotor interaction potential was taken to be:

$$V(r, \Theta) = \frac{C_{12}}{r^{12}} \left[1 + b_1 P_1(\cos\Theta) + b_2 P_2(\cos\Theta)\right] - \frac{C_6}{r^6} \left[1 + a_2 P_2(\cos\Theta)\right], \tag{13}$$

With this choice, the approximation to the quantity $H(\bar{\ell}\bar{\imath};S)$ (Eqs. (XII.72) and (XII.86)) is simply given in terms of the $B_{L\alpha s}$ coefficients of XIV:

$$H(\bar{\ell}\bar{\imath};S) = \eta + \frac{1}{2}\sum_{L\alpha s} B_{L\alpha s}\, D^{L}(\alpha\beta\gamma)_{\alpha s} \tag{14}$$

where η is the elastic phase shift, L indexes the $P_L(\cos\Theta)$ Legendre functions in Eq. (13), and the $D^{L}(S)_{\alpha s}$ are the usual representation coefficients. As given by Eqs. (XIV.23) and (XIV.24), the $B_{L\alpha s}$ are closely related to the generalized action integrals $(S^{(L)}_{n,\alpha,s})$ of Eq. (XIV.25):

$$B_{1\alpha s} = (-1)^{s+1}\left[\frac{16\pi^2}{3\Lambda^*(E^*)^{1/2}}\right] b_1\, S^{(1)}_{12,\alpha,s} \tag{15}$$

$$B_{2\alpha s} = (-1)^{s+1}\left[\frac{16\pi^2}{5\Lambda^*(E^*)^{1/2}}\right]\left[b_2\, S^{(2)}_{12,\alpha,s} - a_2\, S^{(2)}_{6,\alpha,s}\right] \tag{16}$$

where $E^* = E/\epsilon$ is the reduced initial relative translational energy and $\Lambda^* = h/\sigma(2M\epsilon)^{1/2}$ is the de Boer quantum parameter. With these relations, Eq. (14) becomes:

$$H(\bar{\ell}\bar{\imath};S) = \eta + \left[\frac{16\pi^2}{\Lambda^*(E^*)^{1/2}}\right]\hat{H} \tag{17}$$

where

$$\hat{H} = \frac{b_1}{6}\sum_{\alpha s}(-1)^{s+1} S^{(1)}_{12,\alpha,s}\, D^{1}(\alpha\beta\gamma)_{\alpha s} + \frac{1}{10}\sum_{\alpha s}(-1)^{s+1}\left[b_2 S^{(2)}_{12,\alpha,s} - a_2 S^{(2)}_{6,\alpha,s}\right] D^{2}(\alpha\beta\gamma)_{\alpha s} \tag{18}$$

Note that, e.g.,

$$\left(\frac{\partial H}{\partial \alpha}\right) = \left[\frac{16\pi^2}{\Lambda^*(E^*)^{1/2}}\right]\left(\frac{\partial \hat{H}}{\partial \alpha}\right). \tag{19}$$

It is convenient to change the integration variable on the lhs of Eq. (12) from $\Delta\epsilon$ to Δf, the ratio of the change in rotational energy to the initial translational energy. Thus, defining the fraction (initial rotational to initial translational energy)

$$f \equiv E_{rot}/E, \tag{20}$$

it readily follows that in the classical limit

$$f = \frac{\bar{\ell}^2 \Lambda^{*2}}{4\pi^2 E^*}\left(\frac{M\sigma^2}{I}\right) \tag{21}$$

and

$$\Delta f = \frac{(\ell^2 - \bar{\ell}^2)\Lambda^{*2}}{4\pi^2 E^*}\left(\frac{M\sigma^2}{I}\right) = \frac{IkT\Lambda^{*2}}{2\pi^2\hbar^2 E^*}\left(\frac{M\sigma^2}{I}\right)\Delta\epsilon \tag{22}$$

Thus, Eq. (12) becomes

$$\int (\Delta f)^\nu \mathcal{P}(\Delta f)\, d(\Delta f) = \frac{1}{8\pi^2}\left(\frac{M\sigma^2}{I}\right)^\nu \left(\frac{16\pi}{E^*}\right)^{2\nu} \int \hat{K}^\nu(L_a L; S)\, dS \tag{23}$$

where

$$\mathcal{P}(\Delta f) = \frac{2\pi^2\hbar^2}{IkT(\Lambda^*)^2\left(\frac{M\sigma^2}{I}\right)}\,\tilde{\mathcal{P}}(\Delta\epsilon) \tag{24}$$

and, from Eqs. (3) and (19),

$$\hat{K}(L_a L; S) = \left\{\left(\frac{\partial \hat{H}}{\partial \beta}\right)^2 + \frac{1}{\sin^2\beta}\left(\frac{\partial \hat{H}}{\partial \alpha}\right)^2 - 2\frac{\cos\beta}{\sin^2\beta}\left(\frac{\partial \hat{H}}{\partial \alpha}\right)\left(\frac{\partial \hat{H}}{\partial \gamma}\right) - (1 - \cot^2\beta)\left(\frac{\partial \hat{H}}{\partial \gamma}\right)^2 - \left[\frac{(E^*)^2 f}{64\pi^2\left(\frac{M\sigma^2}{I}\right)} - 4\left(\frac{\partial \hat{H}}{\partial \gamma}\right)^2\right]^{1/2} \times \left[\cos\gamma\left(\frac{\partial \hat{H}}{\partial \beta}\right) + \frac{\sin\gamma}{\sin\beta}\left(\frac{\partial \hat{H}}{\partial \alpha}\right) - \cot\beta\sin\gamma\left(\frac{\partial \hat{H}}{\partial \gamma}\right)\right]\right\} \tag{25}$$

In terms of $\hat{H}$ and the reduced variables, the conditions in Eqs. (5) and (6) become:

$$\left|\left(\frac{\partial \hat{H}}{\partial \alpha}\right)\right| < \frac{b^* E^*}{16\pi} \tag{26}$$

$$\left|\left(\frac{\partial \hat{H}}{\partial \gamma}\right)\right| < \frac{E^*}{16\pi}\left[f/\left(\frac{M\sigma^2}{I}\right)\right]^{1/2}. \tag{27}$$

Detailed (but complicated) expressions for the partial derivatives of $\hat{H}$ with respect to α, β and γ follow straightforwardly from Eq. (18); they are displayed in Appendix A. Finally, for computational purposes, it is desirable to remove the apparent singularity of $K(L_a L; S)$ at $\beta = 0$ and π. This is easily accomplished by rearranging Eq. (25) to:

$$\hat{K}(L_a L; S) = \left\{\left(\frac{\partial \hat{H}}{\partial \beta}\right)^2 - \left(\frac{\partial \hat{H}}{\partial \gamma}\right)^2 + \frac{1}{\sin^2\beta}\left[\left(\frac{\partial \hat{H}}{\partial \alpha}\right) - \cos\beta\left(\frac{\partial \hat{H}}{\partial \gamma}\right)\right]^2 - \left[\frac{(E^*)^2 f}{64\pi^2\left(\frac{M\sigma^2}{I}\right)} - 4\left(\frac{\partial \hat{H}}{\partial \gamma}\right)^2\right]^{1/2}\left[\cos\gamma\left(\frac{\partial \hat{H}}{\partial \beta}\right) + \frac{\sin\gamma}{\sin\beta}\left[\left(\frac{\partial \hat{H}}{\partial \alpha}\right) - \cos\beta\left(\frac{\partial \hat{H}}{\partial \gamma}\right)\right]\right]\right\}, \tag{28}$$

where, as is evident from Appendix A, $\frac{1}{\sin\beta}\left[\left(\frac{\partial \hat{H}}{\partial \alpha}\right) - \cos\beta\left(\frac{\partial \hat{H}}{\partial \gamma}\right)\right]$ is finite at $\beta = 0$ and π.

An inversion of the moments can be accomplished by expanding $\mathcal{P}(\Delta f)$ as a Gram-Charlier (type A) series in the Hermite polynomials. Thus, (denoting Δf by x),

$$\mathcal{P}(x) = \frac{1}{(2\pi)^{1/2}\sigma} e^{-(x-\mu)^2/2\sigma^2} \sum_{n=0}^{N} a_n He_n\left(\frac{x-\mu}{\sigma}\right) \tag{29}$$

where μ is the mean value of x, σ^2 is the second moment about the mean, the a_n are expansion coefficients, and the $He_n(y)$ are Hermite polynomials[7] with weight factor $e^{-y^2/2}$. Multiplying Eq. (29) by $He_m\left(\frac{x-\mu}{\sigma}\right)$ and integrating, an expression for the coefficients in the expansion is obtained:

$$a_m = \frac{1}{m!} \int_{-\infty}^{+\infty} He_m\left(\frac{x-\mu}{\sigma}\right) \mathcal{P}(x)\, dx. \qquad (30)$$

As is shown in Appendix B, insertion of explicit forms for the $He_m\left(\frac{x-\mu}{\sigma}\right)$ into Eq. (30) results in simple expressions for the a_m in terms of the moments of $\mathcal{P}(x)$. Thus, within the accuracy of the finite (N+1 term) expansion in Eq. (29), the moments suffice to completely specify the probability density function $\mathcal{P}(\Delta f)$.

As is discussed in detail below, the computational procedure consisted of generating N+1 moments of $\mathcal{P}(\Delta f)$ by use of Eq. (23). These moments, along with Eqs. (29) and (30) were then used to determine $\mathcal{P}(\Delta f)$.

B. Calculations

All computations reported herein were performed on the University of Wisconsin Computing Center Univac 1108. For evaluation of the moments, the method of optimal coefficients[8] was used with $a_2 = 92313$, $a_3 = 24700$, $a_4 = 95582$ and $p = 100063$. This is a quasi-Monte Carlo quadrature technique which offers the advantage that increasing the quadrature size requires merely adding points to the existing lower order quadrature. In order to account for the constraints imposed by the integration limits,

Eqs. (26) and (27), the following procedure was adopted. For each integration point, the values of $\left|\left(\frac{\partial \hat{H}}{\partial \alpha}\right)\right|$ and $\left|\left(\frac{\partial \hat{H}}{\partial \gamma}\right)\right|$ were computed and tested against the appropriate inequalities. If a point violated either constraint, it was rejected and a message to that effect was printed out. In practice, violations were found only in one test case, having a high anisotropy ($b_2 = 1.0$), corresponding to the strong coupling regime. For the calculations presented, the conditions were never violated. As is discussed in Sec. II.C, for the cases investigated, 16,000 integration points and 10 or less moments sufficed to determine $\mathcal{P}(\Delta f)$. Limitations on the accuracy of the moment inversion technique are discussed in Appendix D.

The moments defined in Eq. (23) are functions of a_2, b_1, b_2, E^*, b^*, f and $(M\sigma^2/I)$. In order to make use of the previously computed[1] generalized action integrals, values of the last four parameters were restricted to values compatible with those used in XIV. The corresponding variables in XIV were E^*, b^* and $\zeta\left[\equiv \bar{l}\Lambda^*\left(\frac{M\sigma^2}{I}\right)\right]$. From Eq. (21), it follows that

$$f = \frac{\zeta^2}{4\pi^2\left(\frac{M\sigma^2}{I}\right)E^*} \tag{31}$$

Thus, specification of E^* and ζ fixes the product $\left(\frac{M\sigma^2}{I}\right) f$. For each of three sets of anisotropy parameters ($a_2 = b_2 = 0$, $b_1 = 0.5$; $a_2 = b_1 = 0$, $b_2 = 0.5$; $b_1 = 0$, $a_2 = b_2 = 0.5$), $\mathcal{P}(\Delta f)$ was calculated at $b^* = 0.5, 0.9, 1.0, 1.1, 1.3, 1.5$, for the following combinations: $E^* = 10$, $f = 2/3$, $\frac{M\sigma^2}{I} = 3.42$; $E^* = 3$, $f = 2/3$, $\frac{M\sigma^2}{I} = 5.07$; $E^* = 3$, $f = 3/2$, $\frac{M\sigma^2}{I} = 5.07$.

C. Results

Values of all moments calculated are tabulated in Appendix C. As is evident, in most cases convergence to at least three significant digits was obtained with the 16000 point quadrature. Exceptions occurred primarily for cases having a first moment small in comparison to the square root of the second moment. In such situations, the poorer convergence of (especially) the first moment has only a minor effect on the inverted probability density function. The rate of convergence of the even moments was generally faster than that of the odd moments.

Probability density curves obtained from the inversion procedure are displayed in Figs. 1, 2 and 3. These correspond to the full 10 moment inversions. To test convergence, 6, 7, 8 and 9 moment inversions were also performed for each case. Inspection of the results indicated that in going from 8 to 10 moments, $P(\Delta f)$ values obtained varied less than about 10%.

It is interesting to note that although in all but two cases positive (but small) first moments were obtained (indicating a slight average energy transfer into rotation, i.e., a positive average Δf), the maximum in the $P(\Delta f)$ curves (particularly at low b^*) occurs at negative Δf . This behavior is due to a somewhat slower falloff of P for positive Δf . As would be expected, at large b^* (where first-order perturbation theory is valid) the density functions become more symmetric and sharply peaked. In this region, the second moment dominates and governs the breadth of the curves. A comforting feature of

the results is that although energy conservation limits were not imposed in the inversion procedure, none of the density functions seriously violate the conservation conditions on Δf .

It is of interest to consider the partial inelastic contributions to the total cross section:

$$\frac{d Q(\Delta E_{rot})}{d(\Delta E_{rot})} = \int_0^\infty 2\pi b \, \tilde{P}(\Delta E_{rot}) \, db \tag{32}$$

such that the total inelastic cross section for energy transfer ΔE_{rot} exceeding some arbitrary minimum[9] value, say ΔE_1, is given by

$$Q(|\Delta E_{rot}| > |\Delta E_1|) = \left| \int_{\Delta E_1}^{\Delta E_2} \frac{d Q(\Delta E_{rot})}{d(\Delta E_{rot})} \, d(\Delta E_{rot}) \right| \tag{33}$$

where ΔE_2 is the upper limit imposed by energy conservation. In the notation of Eq. (20), $|\Delta E_2|$ equals E for excitation (transfer of energy into rotation) and E_{rot} for de-excitation (transfer of energy out of rotation). Eqs. (32) and (33) can be written in reduced notation such that

$$Q^*(\Delta f) = Q(\Delta f) / \pi \sigma^2 \tag{34}$$

where σ denotes the usual L.-J. (12,6) size parameter. Thus,

$$\frac{d Q^*(\Delta f)}{d(\Delta f)} = \int_0^\infty 2 b^* P(\Delta f) \, db^*, \tag{35}$$

and

$$Q^*(|\Delta f| > |\Delta f_1|) = \left| \int_{\Delta f_1}^{\Delta f_2} \frac{d Q^*(\Delta f)}{d(\Delta f)} d(\Delta f) \right| . \tag{36}$$

In the insets on the left of each Figure, $2b^* P(\Delta f)$ is plotted vs b^* for three values of $|\Delta f|$. The area under each such curve is the quantity $dQ^*(\Delta f)/d(\Delta f)$ of Eq. (35). It is interesting to note the appearance of the doubly peaked curves in Figs. 3(a) and (b). This behavior has been noted in previous sudden-approximation calculations.[10] Presumably it results from the presence of both attractive and repulsive anisotropies in the interaction potential.

III. DISCUSSION

The results obtained illustrate the computational feasibilty of the classical limit of the "infinite order" GPS method applied to atom-rigid rotor scattering. The procedure for obtaining the moments of the rotational inelasticity probability density function is straightforward. Further, since higher moments involve only integrals of powers of the first moment integrand, the method is economical. The weakest step in the work presented is the moment inversion technique. Although convergent density function curves were obtained in all cases, they resulted from only a finite number of moments of limited accuracy, so they remain somewhat less certain than the moments themselves.

ACKNOWLEDGMENT

The authors acknowledge the benefit of many helpful discussions with Mr. R. A. La Budde on numerical integration and moment inversion techniques.

APPENDIX A

From Eq. (18) and the properties of the representation coefficients, the following expressions are readily obtained:

$$\begin{aligned}\left(\frac{\partial \hat{H}}{\partial \alpha}\right) = &-\frac{1}{3} b_1 \Big\{ S^{(1)}_{12,1,1} \left[\cos\alpha \sin\gamma + \sin\alpha \cos\beta \cos\gamma + \frac{1}{\sqrt{2}} S^{(1)}_{12,0,1} [\sin\alpha \sin\beta]\right] \\ &+ \frac{1}{5}\Big\{ 2\left[b_2 S^{(2)}_{12,2,2} - a_2 S^{(2)}_{6,2,2}\right]\left[\sin\alpha \cos\alpha (1+\cos^2\beta)(1-2\sin^2\gamma) + 2(1-2\sin^2\alpha) \right. \\ &\left. \times \cos\beta \sin\gamma \cos\gamma\right] \\ &+ \left[b_2 S^{(2)}_{12,2,1} - a_2 S^{(2)}_{6,2,1}\right]\left[\sin\alpha \sin\beta \cos\beta (1-2\sin^2\gamma) + 2\cos\alpha \sin\beta \sin\gamma \cos\gamma\right] \\ &+ 2\left[b_2 S^{(2)}_{12,1,2} - a_2 S^{(2)}_{6,1,2}\right]\left[2\sin\alpha \cos\alpha \sin\beta \cos\beta \cos\gamma + (1-2\sin^2\gamma)\sin\beta \sin\gamma\right] \\ &+ \left[b_2 S^{(2)}_{12,1,1} - a_2 S^{(2)}_{6,1,1}\right]\left[\sin\alpha (1-2\cos^2\beta)\cos\gamma - \cos\alpha \cos\beta \sin\gamma\right] \\ &+ 2\left(\frac{3}{2}\right)^{1/2}\left[b_2 S^{(2)}_{12,0,2} - a_2 S^{(2)}_{6,0,2}\right)\left[\sin\alpha \cos\alpha \sin^2\beta\right] \\ &- \left(\frac{3}{2}\right)^{1/2}\left[b_2 S^{(2)}_{12,0,1} - a_2 S^{(2)}_{6,0,1}\right]\left[\sin\alpha \sin\beta \cos\beta\right]\Big\}\end{aligned} \tag{A1}$$

$$\begin{aligned}\left(\frac{\partial \hat{H}}{\partial \beta}\right) = &\frac{1}{6} b_1 \Big\{ -2 S^{(1)}_{12,1,1}\left[\cos\alpha \sin\beta \cos\gamma\right] + \frac{2}{\sqrt{2}} S^{(1)}_{12,1,0}\left[\cos\beta \cos\gamma\right] + \frac{2}{\sqrt{2}} S^{(1)}_{12,0,1}\left[\cos\alpha \cos\beta\right] \\ &+ S^{(1)}_{12,0,0}\left[\sin\beta\right]\Big\} \\ &+ \frac{1}{10}\Big\{ 2\left[b_2 S^{(2)}_{12,2,2} - a_2 S^{(2)}_{6,2,2}\right]\left[(1-2\sin^2\alpha)\sin\beta \cos\beta (1-2\sin^2\gamma) - 4\sin\alpha \cos\alpha \sin\beta \sin\gamma \cos\gamma\right] \\ &- 2\left[b_2 S^{(2)}_{12,2,1} - a_2 S^{(2)}_{6,2,1}\right]\left[\cos\alpha (1-2\sin^2\beta)(1-2\sin^2\gamma) - 2\sin\alpha \cos\beta \sin\gamma \cos\gamma\right] \\ &- 2\left(\frac{3}{2}\right)^{1/2}\left[b_2 S^{(2)}_{12,2,0} - a_2 S^{(2)}_{6,2,0}\right]\left[\sin\beta \cos\beta (1-2\sin^2\gamma)\right] \\ &- 2\left[b_2 S^{(2)}_{12,1,2} - a_2 S^{(2)}_{6,1,2}\right]\left[(1-2\sin^2\alpha)(1-2\sin^2\beta)\cos\gamma - 2\sin\alpha \cos\alpha \cos\beta \sin\gamma\right] \\ &+ 2\left[b_2 S^{(2)}_{12,1,1} - a_2 S^{(2)}_{6,1,1}\right]\left[\sin\alpha \sin\beta \sin\gamma - 4\cos\alpha \sin\beta \cos\beta \cos\gamma\right] \\ &+ 2\left(\frac{3}{2}\right)^{1/2}\left[b_2 S^{(2)}_{12,1,0} - a_2 S^{(2)}_{6,1,0}\right]\left[(1-2\sin^2\beta)\cos\gamma\right] \\ &- 2\left(\frac{3}{2}\right)^{1/2}\left[b_2 S^{(2)}_{12,0,2} - a_2 S^{(2)}_{6,0,2}\right]\left[(1-2\sin^2\alpha)\sin\beta \cos\beta\right] \\ &+ 2\left(\frac{3}{2}\right)^{1/2}\left[b_2 S^{(2)}_{12,0,1} - a_2 S^{(2)}_{6,0,1}\right]\left[\cos\alpha (1-2\sin^2\beta)\right] \\ &+ 3\left[b_2 S^{(2)}_{12,0,0} - a_2 S^{(2)}_{6,0,0}\right]\left[\sin\beta \cos\beta\right]\Big\}\end{aligned} \tag{A2}$$

$$\left(\frac{\partial \hat{H}}{\partial \gamma}\right) = -\frac{1}{3} b_1 \left\{ S^{(1)}_{12,1,1} \left[\sin\alpha\cos\gamma + \cos\alpha\cos\beta\sin\gamma\right] + \frac{1}{\sqrt{2}} S^{(1)}_{12,1,0} \left[\sin\beta\sin\gamma\right] \right\}$$

$$+\frac{1}{5}\left\{ 2\left[b_2 S^{(2)}_{12,2,2} - a_2 S^{(2)}_{6,2,2}\right]\left[(1-2\sin^2\alpha)(1+\cos^2\beta)\sin\gamma\cos\gamma \right.\right.$$

$$\left. + 2\sin\alpha\cos\alpha\cos\beta\,(1-2\sin^2\gamma)\right]$$

$$+2\left[b_2 S^{(2)}_{12,2,1} - a_2 S^{(2)}_{6,2,1}\right]\left[2\cos\alpha\sin\beta\cos\beta\sin\gamma\cos\gamma + \sin\alpha\sin\beta(1-2\sin^2\gamma)\right]$$

$$+2\left(\frac{3}{2}\right)^{1/2}\left[b_2 S^{(2)}_{12,2,0} - a_2 S^{(2)}_{6,2,0}\right]\left[\sin^2\beta\sin\gamma\cos\gamma\right]$$

$$+\left[b_2 S^{(2)}_{12,1,2} - a_2 S^{(2)}_{6,1,2}\right]\left[(1-2\sin^2\alpha)\sin\beta\cos\beta\sin\gamma + 2\sin\alpha\cos\alpha\sin\beta\cos\gamma\right]$$

$$+\left[b_2 S^{(2)}_{12,1,1} - a_2 S^{(2)}_{6,1,1}\right]\left[\cos\alpha(1-2\cos^2\beta)\sin\gamma - \sin\alpha\cos\beta\cos\gamma\right]$$

$$\left. -\left(\frac{3}{2}\right)^{1/2}\left[b_2 S^{(2)}_{12,1,0} - a_2 S^{(2)}_{6,1,0}\right]\left[\sin\beta\cos\beta\sin\gamma\right]\right\}. \qquad \text{(A3)}$$

APPENDIX B

Insertion of explicit forms for the $He_n\left(\frac{X-\mu}{\sigma}\right)$ into Eq. (30) leads directly to the following expressions for the first 11 expansion coefficients in Eq. (29).

$$a_0 = 1 \qquad a_1 = 0 \qquad a_2 = 0$$

$$a_3 = \frac{1}{3!}\left[\frac{\mu_3}{\sigma^3}\right]$$

$$a_4 = \frac{1}{4!}\left[\frac{\mu_4}{\sigma^4} - 3\right]$$

$$a_5 = \frac{1}{5!}\left[\frac{\mu_5}{\sigma^5} - 10\frac{\mu_3}{\sigma^3}\right]$$

$$a_6 = \frac{1}{6!}\left[\frac{\mu_6}{\sigma^6} - 15\frac{\mu_4}{\sigma^4} + 30\right]$$

$$a_7 = \frac{1}{7!}\left[\frac{\mu_7}{\sigma^7} - 21\frac{\mu_5}{\sigma^5} + 105\frac{\mu_3}{\sigma^3}\right]$$

$$a_8 = \frac{1}{8!}\left[\frac{\mu_8}{\sigma^8} - 28\frac{\mu_6}{\sigma^6} + 210\frac{\mu_4}{\sigma^4} - 315\right]$$

$$a_9 = \frac{1}{9!}\left[\frac{\mu_9}{\sigma^9} - 36\frac{\mu_7}{\sigma^7} + 378\frac{\mu_5}{\sigma^5} - 1260\frac{\mu_3}{\sigma^3}\right]$$

$$a_{10} = \frac{1}{10!}\left[\frac{\mu_{10}}{\sigma^{10}} - 45\frac{\mu_8}{\sigma^8} + 630\frac{\mu_6}{\sigma^6} - 3150\frac{\mu_4}{\sigma^4} + 3780\right] \tag{B1}$$

where

$$\mu_n = \int_{-\infty}^{+\infty} (X-\mu)^n P(X)\, dX \tag{B2}$$

and $\sigma^2 = \mu_2$. Expressions for the a's in terms of moments about the origin follow directly from the binomial theorem. Thus, since

$$(X-\mu)^n = \sum_{r=0}^{n} \binom{n}{r} X^r (-\mu)^{n-r}, \tag{B3}$$

$$\mu_n = \int_{-\infty}^{+\infty} (X-\mu)^n P(X)\, dX = \sum_{r=0}^{n} \binom{n}{r} (-M_1)^{n-r} M_r \tag{B4}$$

where

$$M_1 = \mu = \int_{-\infty}^{+\infty} x \, P(x) \, dx$$

$$M_r = \int_{-\infty}^{+\infty} x^r \, P(x) \, dx \, . \qquad \text{(B5)}$$

APPENDIX C

For computational purposes, Eq. (23) has been rewritten in the form:

$$M_n = \frac{1}{8\pi^2} \int \left\{ \left[\frac{M G^2}{I} \right] \left[\frac{16\pi}{E^*} \right]^2 K(L_a L; S) \right\}^n dS \qquad \text{(C1)}$$

where M_n is the n^{th} moment of the probability density function. Tables 1, 2 and 3 list values[11] obtained for the M_n. The final digit of each entry is believed to be significant. Note that $M_o = 1$ throughout.

TABLE 1† Computed Moments (M_n) for $a_2 = b_2 = 0$, $b_1 = 0.5$

$E^* = 10$, $f = 2/3$, $\frac{M\mathfrak{G}^2}{I} = 3.42$

n \ b*	0.5	0.9	1.0	1.1	1.3	1.5
1	0.618 (-2)	0.7931 (-2)	0.543 (-2)	0.225 (- 2)	0.60 (- 4)	0.1 (- 5)
2	0.3487 (-1)	0.1417 (-1)	0.8058 (-2)	0.3083 (- 2)	0.8907 (- 4)	0.2163 (- 5)
3	0.2032 (-2)	0.4730 (-3)	0.1676 (-3)	0.259 (- 4)	0.22 (- 7)	0.11 (-10)
4	0.2283 (-2)	0.3718 (-3)	0.1202 (-3)	0.1778 (- 4)	0.1537 (- 7)	0.9194 (-11)
5	0.2792 (-3)	0.2300 (-4)	0.4557 (-5)	0.2740 (- 6)	0.71 (-11)	0.10 (-15)
6	0.1867 (-3)	0.1196 (-4)	0.2197 (-5)	0.1265 (- 6)	0.3347 (-11)	0.4978 (-16)
7	0.3403 (-4)	0.1073 (-5)	0.1212 (-6)	0.2885 (- 8)	0.238 (-14)	0.8 (-21)
8	0.1734 (-4)	0.4309 (-6)	0.4492 (-7)	0.1011 (- 8)	0.8300 (-15)	0.3079 (-21)
9	0.4017 (-5)	0.4961 (-7)	0.3223 (-8)	0.3067 (-10)	0.81 (-18)	0.71 (-26)
10	0.1751 (-5)	0.1674 (-7)	0.9908 (-9)	0.8745 (-11)	0.2235 (-18)	0.2072 (-26)

$E^* = 3$, $f = 2/3$, $\frac{M\mathfrak{G}^2}{I} = 5.07$

n \ b*	0.5	0.9	1.0	1.1	1.3	1.5
1	0.1 (-3)	0.1917 (-1)	0.2698 (-1)	0.3010 (-1)	0.78 (-2)	0.6 (- 4)
2	0.1239 (0)	0.8257 (-1)	0.6822 (-1)	0.5164 (-1)	0.1237 (-1)	0.1148 (- 3)
3	0.2077 (-1)	0.1209 (-1)	0.9538 (-2)	0.6317 (-2)	0.403 (-3)	0.35 (- 7)
4	0.3095 (-1)	0.1362 (-1)	0.9249 (-2)	0.5241 (-2)	0.3054 (-3)	0.2773 (- 7)
5	0.1155 (-1)	0.3943 (-2)	0.2403 (-2)	0.1136 (-2)	0.1913 (-4)	0.174 (-10)
6	0.1051 (-1)	0.2964 (-2)	0.1634 (-2)	0.6861 (-3)	0.9811 (-5)	0.8787 (-11)
7	0.5534 (-2)	0.1190 (-2)	0.580 (-3)	0.2019 (-3)	0.918 (-6)	0.88 (-14)
8	0.4235 (-2)	0.755 (-3)	0.3361 (-3)	0.1042 (-3)	0.3682 (-6)	0.3212 (-14)
9	0.2608 (-2)	0.358 (-3)	0.1411 (-3)	0.3650 (-4)	0.451 (-7)	0.45 (-17)
10	0.1878 (-2)	0.2112 (-3)	0.760 (-4)	0.1741 (-4)	0.1533 (-7)	0.1278 (-17)

Table 1 Continued

$E^* = 3$, $f = 3/2$, $\frac{M\sigma^2}{I} = 5.07$

n \ b^*	0.5	0.9	1.0	1.1	1.3	1.5
1	0.3898 (-1)	0.8 (-3)	0.82 (-2)	0.1823 (-1)	0.42 (-2)	0.2 (- 4)
2	0.2582 (0)	0.1642 (0)	0.1311 (0)	0.9443 (-1)	0.1820 (-1)	0.1150 (- 3)
3	0.5777 (-1)	0.1663 (-1)	0.1249 (-1)	0.864 (-2)	0.382 (-3)	0.15 (- 7)
4	0.1284 (0)	0.5056 (-1)	0.3240 (-1)	0.1698 (-1)	0.6914 (-3)	0.3031 (- 7)
5	0.5521 (-1)	0.1197 (-1)	0.674 (-2)	0.3037 (-2)	0.299 (-4)	0.88 (-11)
6	0.8130 (-1)	0.1955 (-1)	0.1005 (-1)	0.3849 (-2)	0.3458 (-4)	0.1067 (-10)
7	0.4922 (-1)	0.7244 (-2)	0.3218 (-2)	0.1023 (-2)	0.235 (-5)	0.50 (-14)
8	0.5904 (-1)	0.8655 (-2)	0.3570 (-2)	0.1001 (-2)	0.2009 (-5)	0.4330 (-14)
9	0.4338 (-1)	0.4205 (-2)	0.1498 (-2)	0.345 (-3)	0.186 (-6)	0.288 (-17)
10	0.4674 (-1)	0.4207 (-2)	0.1393 (-2)	0.286 (-3)	0.1282 (-6)	0.1907 (-17)

† Numbers in parentheses represent the power of ten by which each entry is to be multiplied.

TABLE 2 Computed Moments (M_n) for $a_2 = b_1 = 0$, $b_2 = 0.5$

$E^* = 10$, $f = 2/3$, $\frac{M\sigma^2}{I} = 3.42$

n \ b^*	0.5	0.9	1.0	1.1	1.3	1.5
1	0.839 (-2)	0.1118 (-1)	0.734 (-2)	0.283 (-2)	0.698 (- 4)	0.190 (- 5)
2	0.5299 (-1)	0.1872 (-1)	0.9882 (-2)	0.3418 (-2)	0.7769 (- 4)	0.1484 (- 5)
3	0.561 (-2)	0.1092 (-2)	0.3568 (-3)	0.499 (-4)	0.315 (- 7)	0.1561 (-10)
4	0.661 (-2)	0.8608 (-3)	0.2520 (-3)	0.3295 (-4)	0.1961 (- 7)	0.743 (-11)
5	0.1504 (-2)	0.989 (-4)	0.1806 (-4)	0.976 (-6)	0.162 (-10)	0.147 (-15)
6	0.1112 (-2)	0.5409 (-4)	0.894 (-5)	0.4469 (-6)	0.695 (-11)	0.522 (-16)
7	0.368 (-3)	0.913 (-5)	0.961 (-6)	0.2029 (-7)	0.90 (-14)	0.17 (-20)
8	0.2218 (-3)	0.4057 (-5)	0.380 (-6)	0.718 (-8)	0.2867 (-14)	0.4278 (-21)
9	0.897 (-4)	0.868 (-6)	0.530 (-7)	0.439 (-9)	0.53 (-17)	0.24 (-25)
10	0.492 (-4)	0.341 (-6)	0.181 (-7)	0.1276 (-9)	0.1292 (-17)	0.3825 (-26)

$E^* = 3$, $f = 2/3$, $\frac{M\sigma^2}{I} = 5.07$

n \ b^*	0.5	0.9	1.0	1.1	1.3	1.5
1	- 0.88 (-2)	+ 0.223 (-1)	0.3450 (-1)	0.389 (-1)	0.814 (-2)	0.45 (- 4)
2	+ 0.1847 (0)	0.1077 (0)	0.8468 (-1)	0.6042 (-1)	0.1098 (-1)	0.5543 (- 4)
3	0.5188 (-1)	0.2609 (-1)	0.1944 (-1)	0.1203 (-1)	0.553 (-3)	0.174 (- 7)
4	0.8902 (-1)	0.3187 (-1)	0.2012 (-1)	0.1045 (-1)	0.4015 (-3)	0.1144 (- 7)
5	0.5723 (-1)	0.1582 (-1)	0.895 (-2)	0.3871 (-2)	0.414 (-4)	0.74 (-11)
6	0.650 (-1)	0.1424 (-1)	0.722 (-2)	0.2718 (-2)	0.2139 (-4)	0.329 (-11)
7	0.562 (-1)	0.954 (-2)	0.430 (-2)	0.1343 (-2)	0.326 (-5)	0.32 (-14)
8	0.582 (-1)	0.7985 (-2)	0.324 (-2)	0.8763 (-3)	0.1372 (-5)	0.1100 (-14)
9	0.563 (-1)	0.6074 (-2)	0.221 (-2)	0.4970 (-3)	0.266 (-6)	0.146 (-17)
10	0.578 (-1)	0.5037 (-2)	0.165 (-2)	0.3184 (-3)	0.9866 (-7)	0.401 (-18)

Table 2 Continued

$E^* = 3$, $f = 3/2$, $\frac{M\epsilon^2}{I} = 5.07$

n \ b^*	0.5	0.9	1.0	1.1	1.3	1.5
1	+ 0.4746 (-1)	- 0.113 (-1)	+ 0.7 (-3)	0.161 (-1)	0.267 (-2)	0.4 (- 5)
2	0.3294 (0)	+ 0.1694 (0)	0.1197 (0)	0.7410 (-1)	0.775 (-2)	0.1115 (- 4)
3	0.1084 (0)	0.187 (-1)	0.1297 (-1)	0.8195 (-2)	0.137 (-1)	0.31 (- 9)
4	0.2545 (0)	0.698 (-1)	0.3737 (-1)	0.1567 (-1)	0.2096 (-3)	0.4920 (- 9)
5	0.1643 (0)	0.220 (-1)	0.1040 (-1)	0.3763 (-2)	0.77 (-5)	0.31 (-13)
6	0.2675 (0)	0.403 (-1)	0.167 (-1)	0.481 (-2)	0.796 (-5)	0.3005 (-13)
7	0.2395 (0)	0.212 (-1)	0.75 (-2)	0.177 (-2)	0.449 (-6)	0.318 (-17)
8	0.335 (0)	0.288 (-1)	0.91 (-2)	0.181 (-2)	0.353 (-6)	0.2128 (-17)
9	0.354 (0)	0.202 (-1)	0.54 (-2)	0.86 (-3)	0.266 (-7)	0.32 (-21)
10	0.466 (0)	0.236 (-1)	0.57 (-2)	0.77 (-3)	0.1713 (-7)	0.1640 (-21)

Table 3 Computed Moments (M_n) for $b_1 = 0$, $a_2 = b_2 = 0.5$

$E^* = 10$, $f = 2/3$, $\frac{M\sigma^2}{I} = 3.42$

n \ b^*	0.5	0.9	1.0	1.1	1.3	1.5
1	0.161 (-2)	0.215 (- 3)	0.4869 (- 3)	0.1129 (- 2)	0.584 (- 3)	0.103 (- 3)
2	0.5361 (-2)	0.7879 (- 3)	0.1010 (- 2)	0.1613 (- 2)	0.6909 (- 3)	0.995 (- 4)
3	0.6835 (-4)	0.156 (- 5)	0.403 (- 5)	0.1479 (- 4)	0.2907 (- 5)	0.660 (- 7)
4	0.6587 (-4)	0.1538 (- 5)	0.3008 (- 5)	0.1022 (- 4)	0.1898 (- 5)	0.391 (- 7)
5	0.1845 (-5)	0.787 (- 8)	0.2894 (- 7)	0.1985 (- 6)	0.1639 (- 7)	0.5167 (-10)
6	0.1057 (-5)	0.4467 (- 8)	0.1367 (- 7)	0.9213 (- 7)	0.729 (- 8)	0.2136 (-10)
7	0.474 (-7)	0.398 (-10)	0.2127 (- 9)	0.2749 (- 8)	0.963 (-10)	0.426 (-13)
8	0.1968 (-7)	0.1589 (-10)	0.749 (-10)	0.9734 (- 9)	0.3263 (-10)	0.1358 (-13)
9	0.1215 (-8)	0.203 (-12)	0.1594 (-11)	0.389 (-10)	0.5771 (-12)	0.356 (-16)
10	0.4044 (-9)	0.631 (-13)	0.452 (-12)	0.1128 (-10)	0.1599 (-12)	0.942 (-17)

$E^* = 3$, $f = 2/3$, $\frac{M\sigma^2}{I} = 5.07$

n \ b^*	0.5	0.9	1.0	1.1	1.3	1.5
1	0.277 (- 2)	0.131 (-2)	0.268 (-2)	0.624 (-2)	0.928 (-2)	0.104 (- 2)
2	0.2523 (- 2)	0.4557 (-2)	0.6988 (-2)	0.1043 (-1)	0.1269 (-1)	0.1099 (- 2)
3	0.3924 (- 4)	0.494 (-4)	0.1821 (-3)	0.5567 (-3)	0.9438 (-3)	0.813 (- 5)
4	0.2225 (- 4)	0.5660 (-4)	0.1670 (-3)	0.4227 (-3)	0.696 (-3)	0.5050 (- 5)
5	0.668 (- 6)	0.1560 (-5)	0.1025 (-4)	0.4725 (-4)	0.1059 (-3)	0.766 (- 7)
6	0.2766 (- 6)	0.1048 (-5)	0.5918 (-5)	0.2503 (-4)	0.577 (-4)	0.335 (- 7)
7	0.1221 (- 7)	0.493 (-7)	0.571 (-6)	0.411 (-5)	0.1269 (-4)	0.755 (- 9)
8	0.403 (- 8)	0.2350 (-7)	0.2496 (-6)	0.1771 (-5)	0.586 (-5)	0.261 (- 9)
9	0.232 (- 9)	0.1567 (-8)	0.3205 (-7)	0.367 (-6)	0.159 (-5)	0.81 (-11)
10	0.645 (-10)	0.587 (-9)	0.1167 (-7)	0.1396 (-6)	0.670 (-6)	0.225 (-11)

Table 3 Continued

$E^* = 3,\ f = 1.5,\ \frac{Mc^2}{I} = 5.07$

n \ b*	0.5	0.9	1.0	1.1	1.3	1.5
1	0.367 (-2)	0.4101 (-2)	0.205 (-2)	0.30 (- 3)	0.63 (- 3)	0.23 (- 4)
2	0.2002 (-1)	0.6304 (-2)	0.3921 (-2)	0.2877 (- 2)	0.1290 (- 2)	0.3563 (- 4)
3	0.4786 (-3)	0.1172 (-3)	0.376 (-4)	0.834 (- 5)	0.509 (- 5)	0.35 (- 8)
4	0.9361 (-3)	0.1255 (-3)	0.437 (-4)	0.1803 (- 4)	0.615 (- 5)	0.4994 (- 8)
5	0.478 (-4)	0.429 (-5)	0.84 (-6)	0.119 (- 6)	0.54 (- 7)	0.12 (-11)
6	0.5773 (-4)	0.349 (-5)	0.728 (-6)	0.1488 (- 6)	0.480 (- 7)	0.1200 (-11)
7	0.467 (-5)	0.172 (-6)	0.207 (-7)	0.158 (- 8)	0.65 (- 9)	0.4 (-15)
8	0.4142 (-5)	0.113 (-6)	0.1450 (-7)	0.1414 (- 8)	0.457 (- 9)	0.354 (-15)
9	0.460 (-6)	0.72 (-8)	0.541 (-9)	0.210 (-10)	0.83 (-11)	0.14 (-18)
10	0.3275 (-6)	0.401 (-8)	0.317 (-9)	0.1460 (-10)	0.481 (-11)	0.115 (-18)

APPENDIX D

The problems inherent in obtaining accurate probability density functions from a knowledge of the first several moments are illustrated in Fig. 4. Shown are 7 and 10 moment inversions obtained (via Eqs. (29) and (30)) from the exact moments of the indicated rectangular $P(\Delta f)$ (6, 8 and 9 moment inversions are similar). Although the two approximate distributions agree to within ca. $\pm$ 20% everywhere, neither provides a particularly accurate representation of the rectangular function. This behavior of relatively slow convergence beyond some level appears to be characteristic of moment inversion techniques when the function whose moments are to be inverted differs markedly from the zeroth-order form (e.g., a Gaussian for the Gram-Charlier series).

The implication of Fig. 4 in the present context is to caution against a too strict interpretation of the $P(\Delta f)$ curves presented in Figs. 1-3. Thus, although reasonably convergent moment inversions were obtained in all cases, the 10 moment inversion P curves may still not accurately represent the true probability density functions. However, since a consistent inversion technique was used throughout, it is believed that at least the qualitative trends of P with b^*, E^*, etc. are properly represented.

FOOTNOTES

1. M. D. Pattengill, C. F. Curtiss and R. B. Bernstein, J. Chem. Phys. 54, 2197 (1971).

2. C. F. Curtiss, J. Chem. Phys. 52, 4832 (1970), paper XII of this series.

3. "High" implies initial rotor states ($\bar{\ell}$) such that $\bar{\ell}(\bar{\ell}+1)$ is well approximated by $\bar{\ell}^2$.

4. C. F. Curtiss, J. Chem. Phys. 54, 872 (1971), paper I; C. F. Curtiss, J. Chem. Phys. (in press), paper II; R. Olmsted and C. F. Curtiss, Report WIS-TCI-424, Theoretical Chemistry Institute, University of Wisconsin, 6 November 1970, paper III.

5. The term "infinite-order" indicates that the full exponential in the expression for $\mathcal{S}(\bar{\ell}\bar{\lambda};S)$ (cf. Eq. (4)) has been retained. As noted in Ref. 2, the expression used here (even with retention of the full exponential) for the classical limit of $\mathcal{H}(\bar{\ell}\bar{\lambda};S)$ is valid only to first-order in the anisotropic portion of the interaction potential.

6. Eq. (T.II.27) denotes Eq. (27) of paper II of the transport properties series (Ref. 4), etc. Eq. (XIV.25) denotes Eq. (25) of paper XIV of the present series.

7. Handbook of Mathematical Functions, edited by M. Abramowitz and I. A. Stegun, National Bureau of Standards, Washington, D. C., 1964.

8. M. Klerer and G. A. Korn, eds., Digital Computer User's Handbook, McGraw-Hill, New York, 1967, Sec. 2.5-11.

9. It may be shown that $\frac{dQ(\Delta E_{rot})}{d(\Delta E_{rot})}$ becomes infinite as ΔE_{rot} approaches zero in such a manner that the integral (of Eq. (33)) over all ΔE_{rot} diverges. This is closely related to the well-known divergence of the classical elastic differential cross sections as $\chi \to 0$.

10. R. W. Fenstermaker and R. B. Bernstein, J. Chem. Phys. 47, 4417 (1967).

11. It has been shown that for the potentials investigated, M_2 in the limit of large b^* can be obtained by evaluation of the *lhs* of Eq. (7) using the first-order semiclassical $P(\bar{l}; l; \bar{\lambda})$ of paper XIV. The values obtained here and in paper XIV are consistent with this result (numerical agreement to about three significant figures). In some cases, agreement persists to surprisingly low values of b^*.

FIGURE LEGENDS

Figure 1. $P(\Delta f)$ vs. Δf at various b^* for anisotropy parameters $a_2 = b_2 = 0$, $b_1 = 0.5$: (a) $E^* = 10$, $f = 0.67$, $\frac{M\sigma^2}{I} = 3.42$; (b) $E^* = 3$, $f = 0.67$, $\frac{M\sigma^2}{I} = 5.07$; (c) $E^* = 3$, $f = 1.5$, $\frac{M\sigma^2}{I} = 5.07$. Curves in the main portion of each frame correspond to $b^* = 0.5$, 0.9, 1.0, 1.1 and 1.3. The marks on the abscissae at $\Delta f = -0.67$ or -1.5, and 1.0 indicate conservation limits. For comparison with a quantum calculation, small marks around $\Delta f = 0$ indicate Δf values corresponding to unit changes in the rotor quantum number for $\Lambda^* = 0.1$ (changes corresponding to $\Delta \ell = \pm 1, \pm 2, \ldots, \pm 5$ are shown). Curves in the insets to the right of each frame correspond to $b^* = 1.3$ and 1.5 (dashed curves are simple Gaussians computed from the second moments, for $b^* = 1.5$). Insets to the left give $2b^* P(\Delta f)$ vs. b^* for the indicated values of Δf (dashed curves correspond to negative Δf, solid curves to positive Δf).

Figure 2. Same as Figure 1 for $a_2 = b_1 = 0$, $b_2 = 0.5$.

Figure 3. Same as Figure 1 for $b_1 = 0$, $a_2 = b_2 = 0.5$. Note that only curves corresponding to $b^* = 0.5$, 0.9, 1.0, and 1.1 are plotted in the main portion of each frame.

Figure 4. Inversions obtained from the first 7 and first 10 moments of the indicated rectangular probability density function.

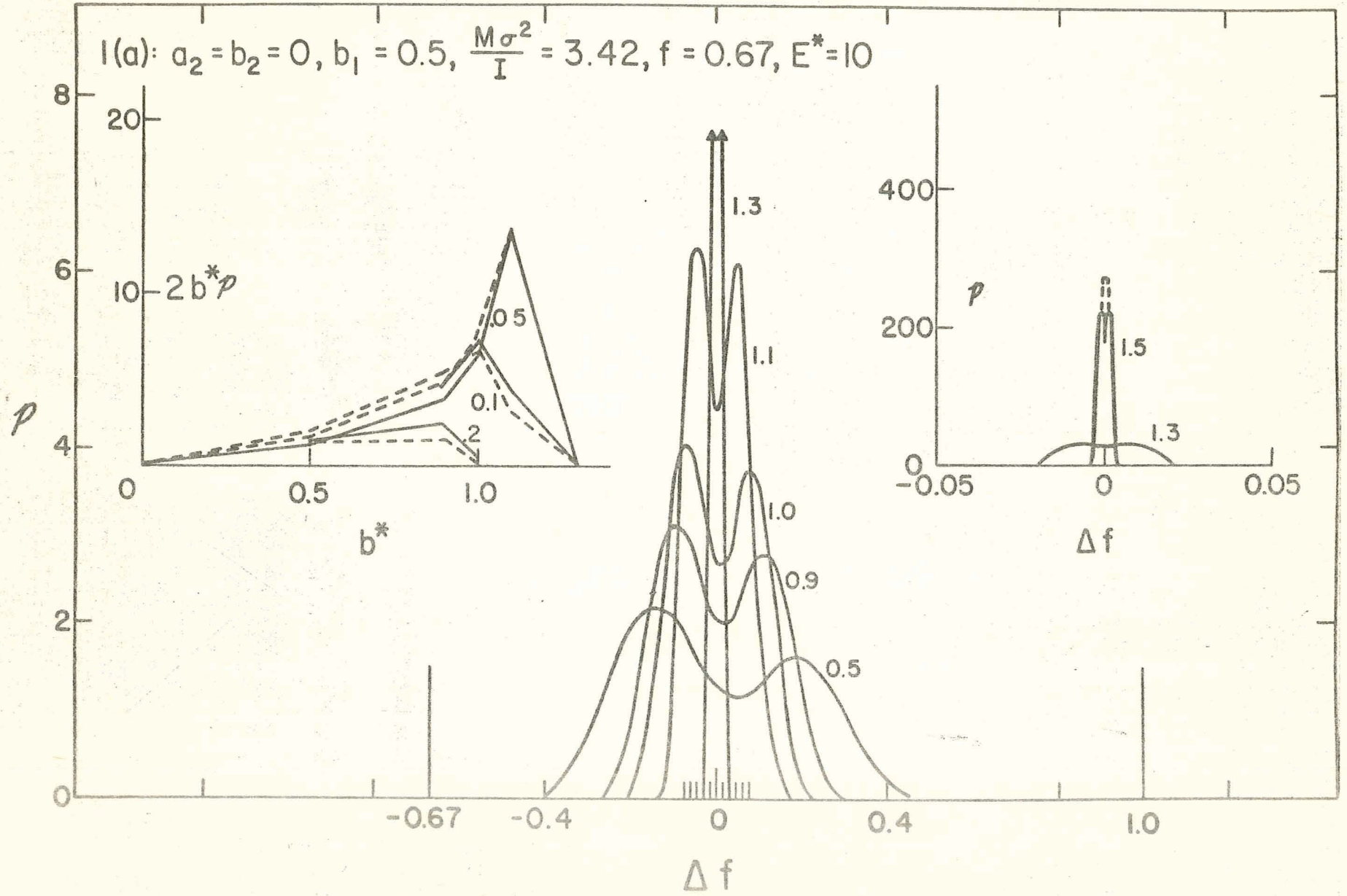
1(a): $a_2 = b_2 = 0$, $b_1 = 0.5$, $\frac{M\sigma^2}{I} = 3.42$, $f = 0.67$, $E^* = 10$
p
Δf
$2b^*p$
b^*
0.5
0.1
.2
1.3
1.1
1.0
0.9
0.5
1.5
1.3
8
6
4
2
0
20
10
400
200
0
0.5
1.0
-0.67
-0.4
0.4
1.0
-0.05
0.05

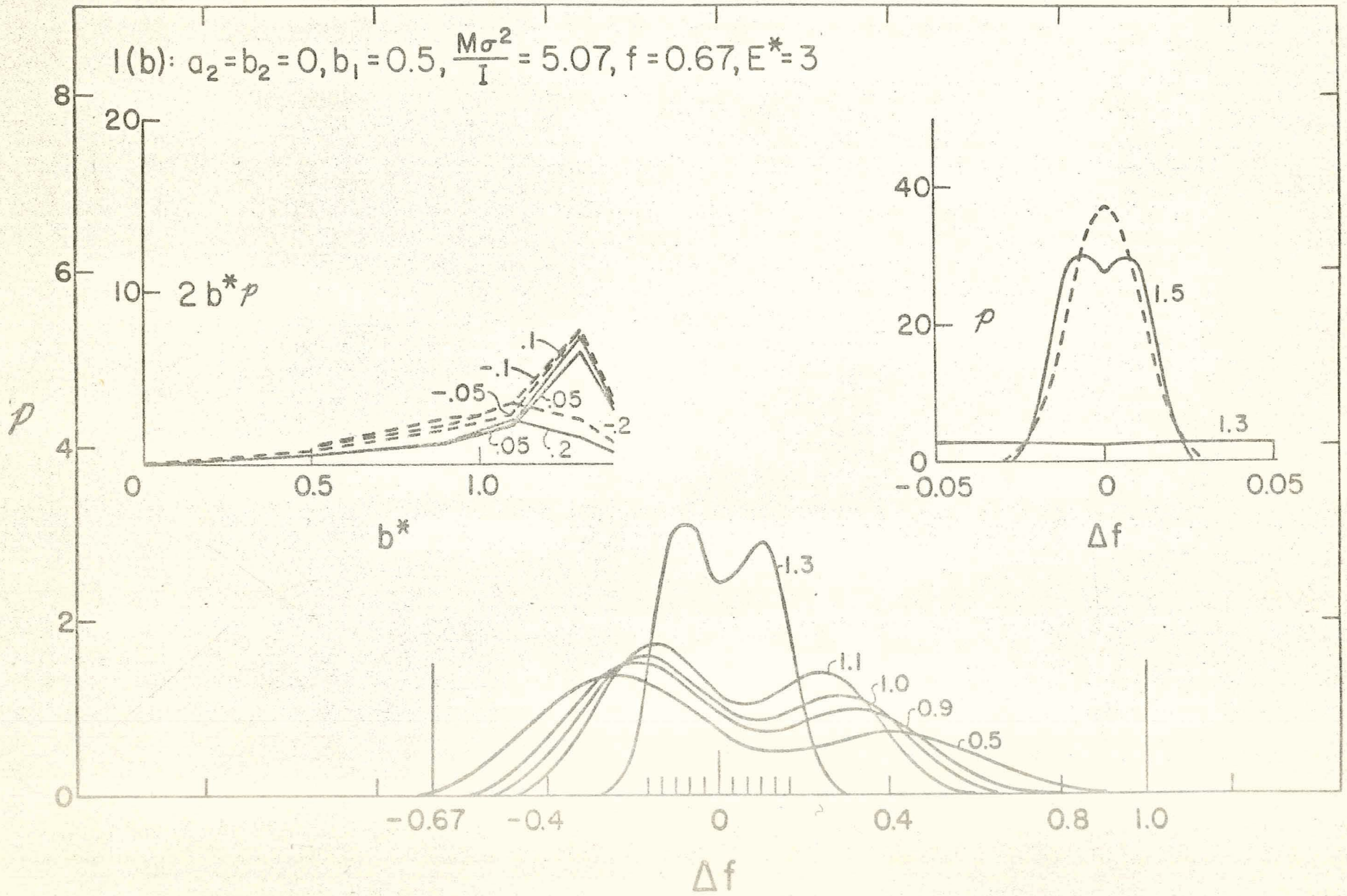
1(b): $a_2 = b_2 = 0, b_1 = 0.5, \frac{M\sigma^2}{I} = 5.07, f = 0.67, E^* = 3$
$2\,b^* p$
p
b^*
.1
-.1
-.05
.05
-.2
.05
.2
Δf
1.5
1.3
1.3
1.1
1.0
0.9
0.5
Δf

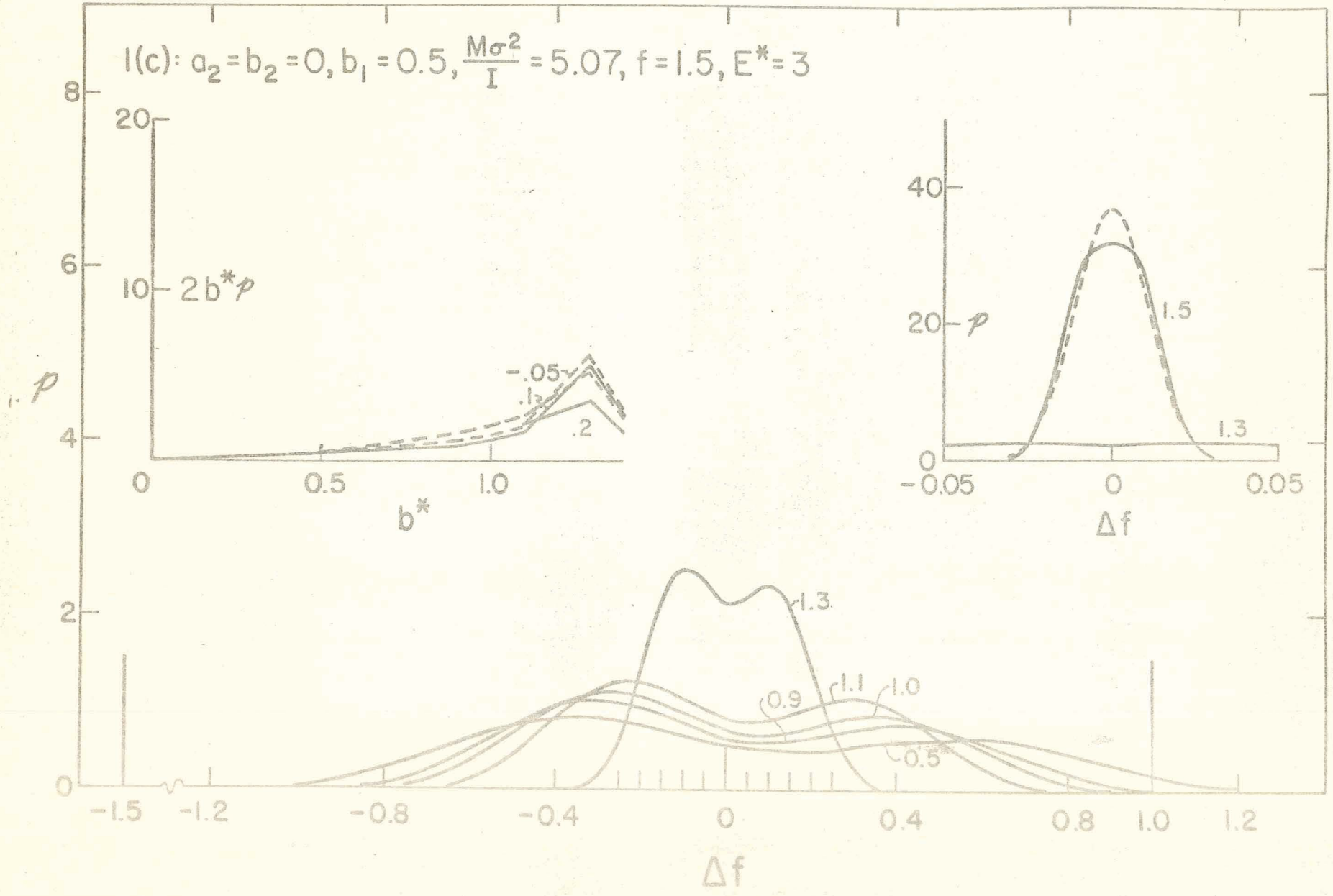
I(c): $a_2 = b_2 = 0, b_1 = 0.5, \frac{M\sigma^2}{I} = 5.07, f = 1.5, E^* = 3$
p
$2b^*p$
b^*
Δf
-.05
.1
.2
1.5
1.3
1.1
1.0
0.9
0.5

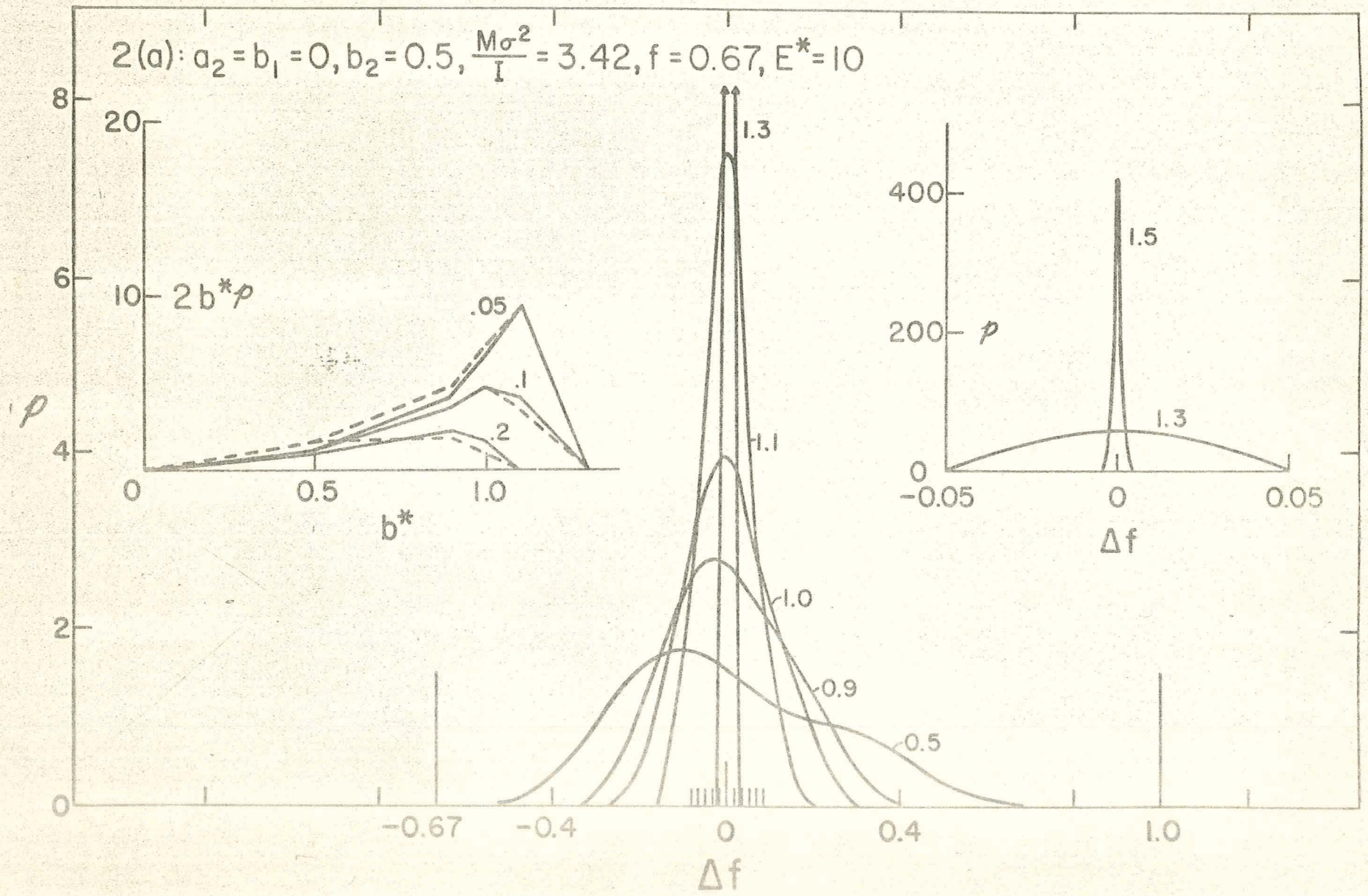
2(a): $a_2 = b_1 = 0, b_2 = 0.5, \frac{M\sigma^2}{I} = 3.42, f = 0.67, E^* = 10$
p
Δf
1.3
1.1
1.0
0.9
0.5
2b*p
.05
.1
.2
b*
1.5
1.3
1
Δf

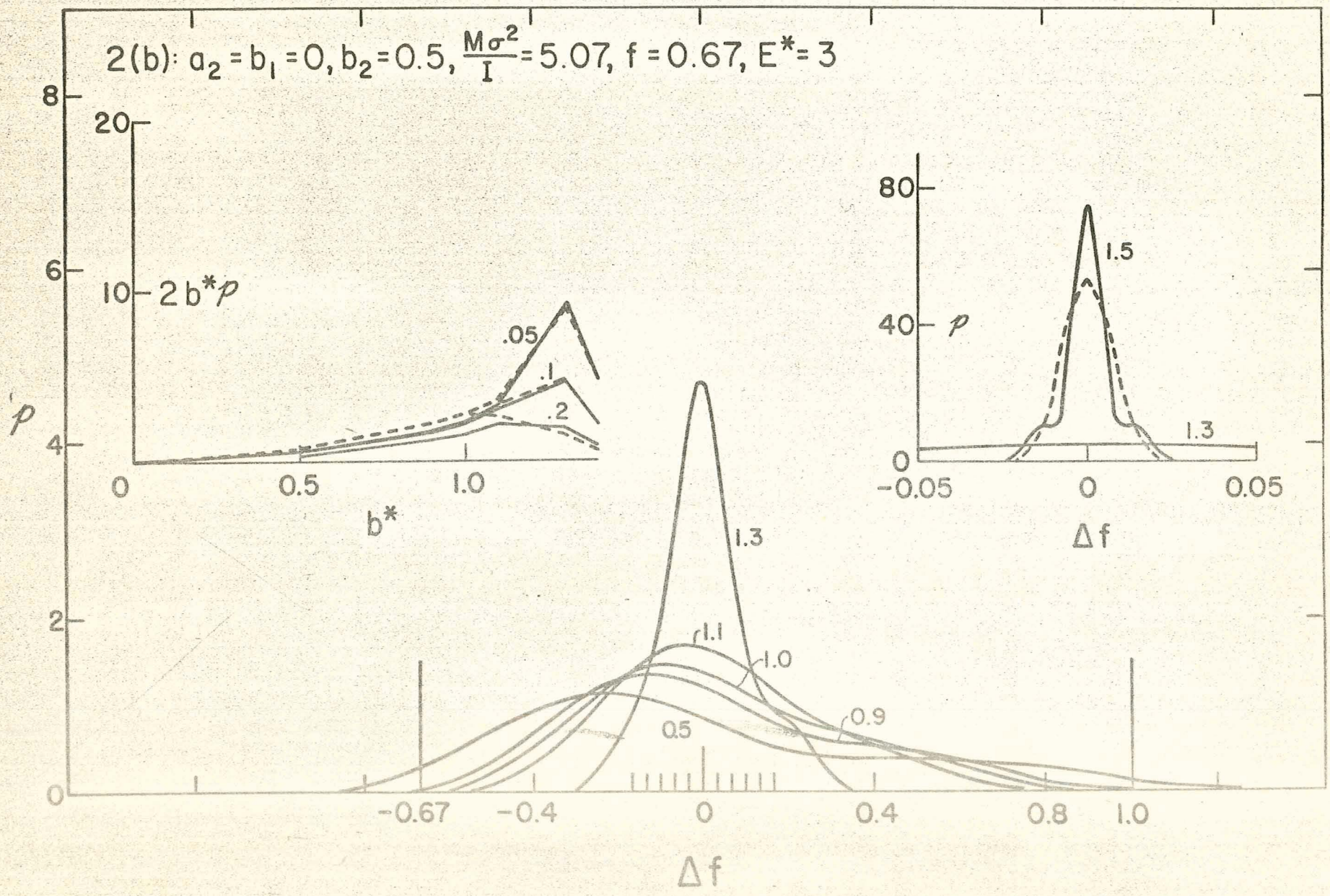
2(b): $a_2 = b_1 = 0, b_2 = 0.5, \frac{M\sigma^2}{I} = 5.07, f = 0.67, E^* = 3$
p
8
6
4
2
0
-0.67
-0.4
0
0.4
0.8
1.0
Δf
1.3
1.1
1.0
0.9
0.5
20
10
2b*p
.05
.1
.2
0
0.5
1.0
b*
80
40
p
1.5
1.3
0
-0.05
0
0.05
Δf

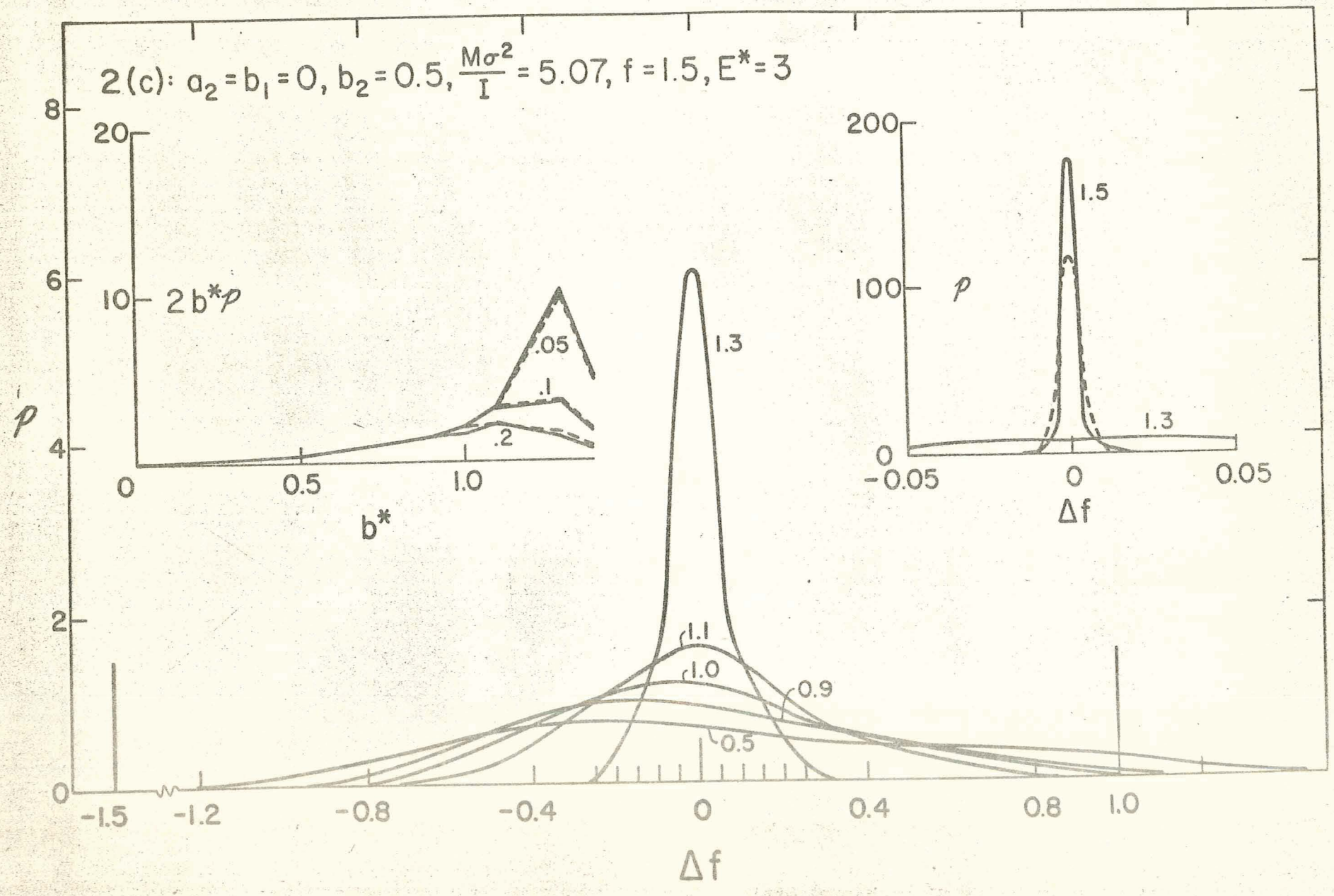
2(c): $a_2 = b_1 = 0$, $b_2 = 0.5$, $\frac{M\sigma^2}{I} = 5.07$, $f = 1.5$, $E^* = 3$
p
Δf
$2b^*p$
b^*
p
Δf
1.5
1.3
1.1
1.0
0.9
0.5
.05
.1
.2
1.3

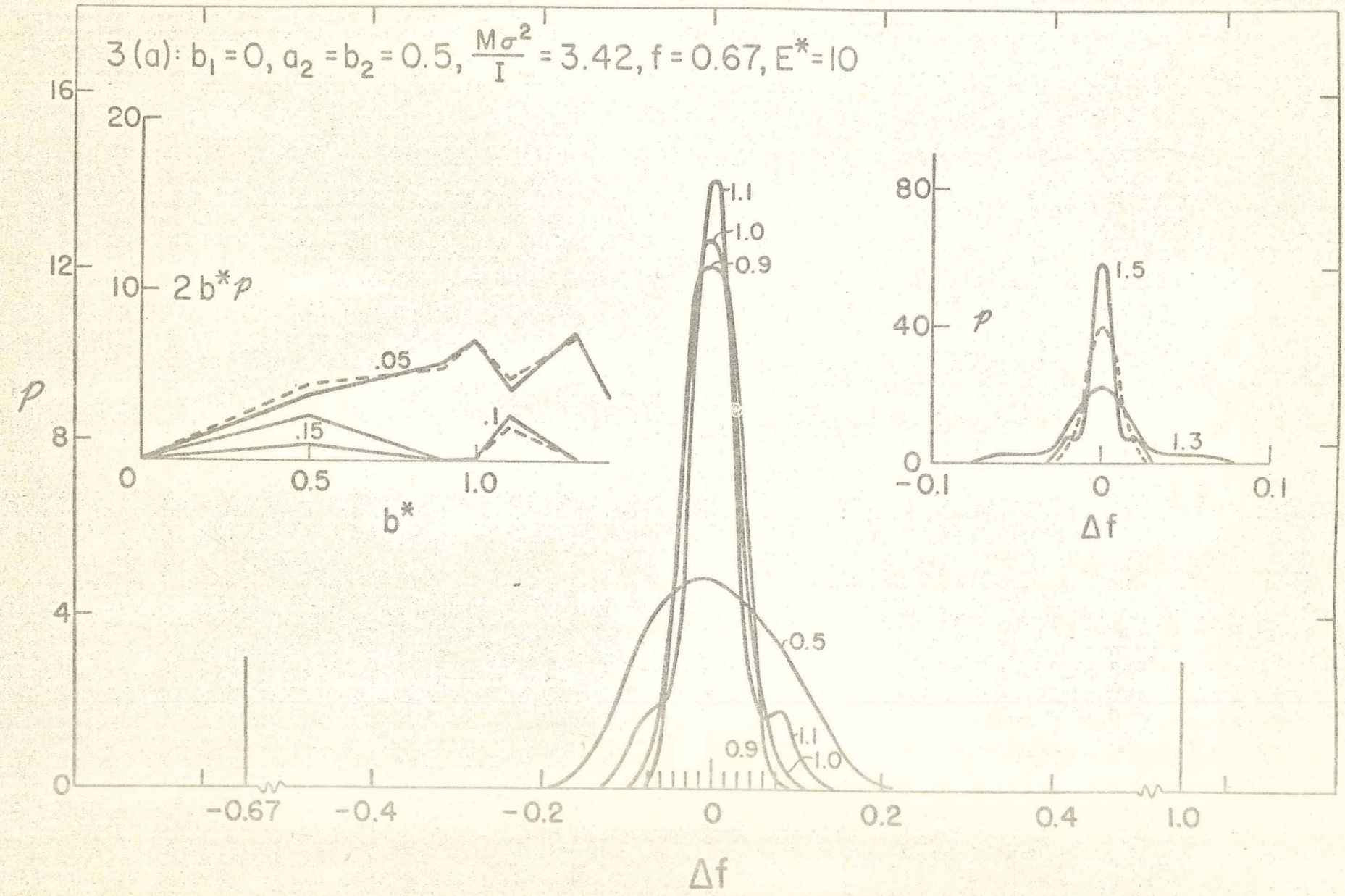
3(a): $b_1 = 0$, $a_2 = b_2 = 0.5$, $\frac{M\sigma^2}{I} = 3.42$, $f = 0.67$, $E^* = 10$
p
Δf
$2b^*p$
b^*
.05
.15
.1
1.1
1.0
0.9
0.5
1.5
1.3
16
12
8
4
0
20
10
80
40
-0.67
-0.4
-0.2
0.2
0.4
1.0
-0.1
0.1

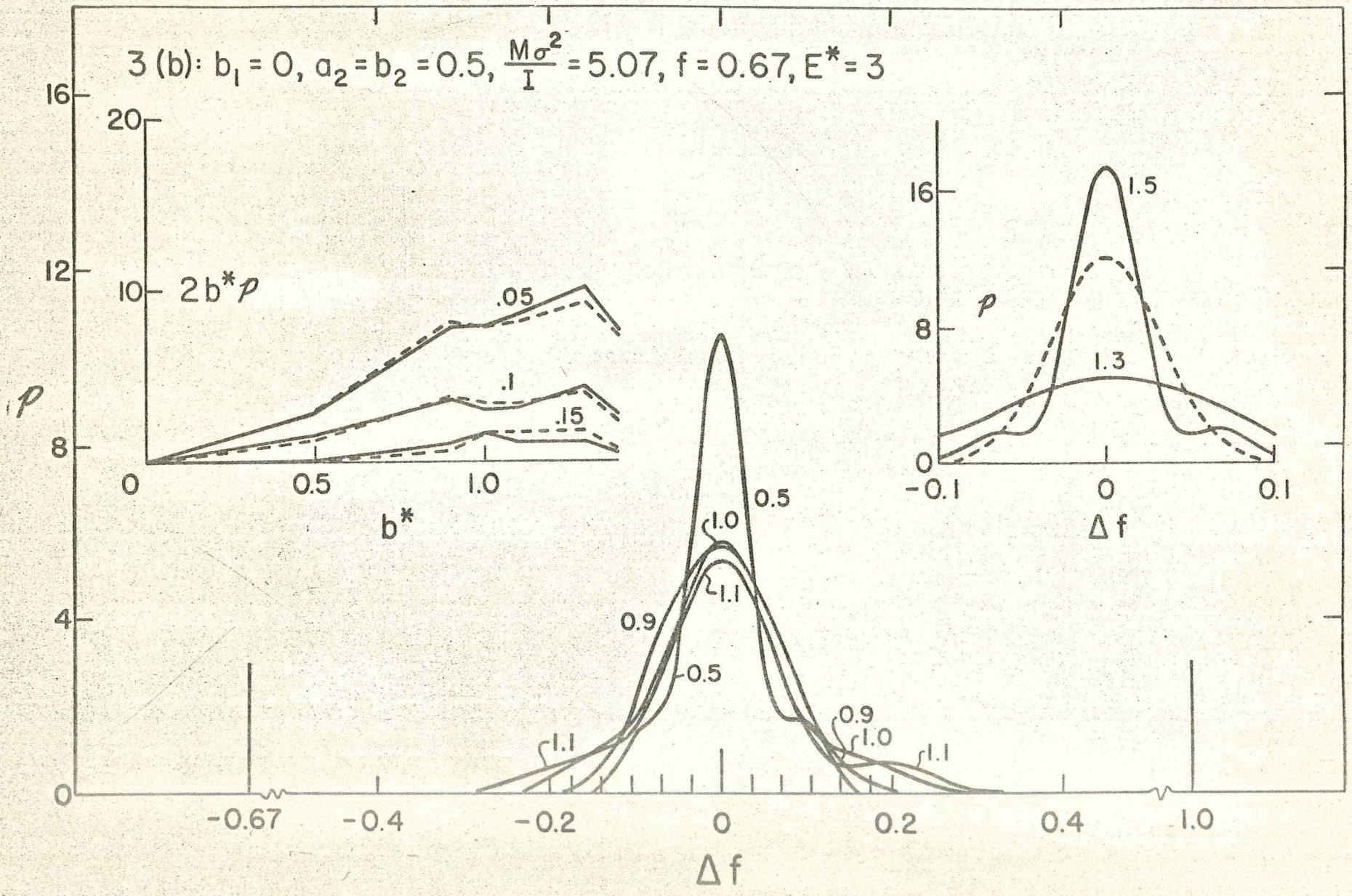
3 (b): $b_1 = 0$, $a_2 = b_2 = 0.5$, $\frac{M\sigma^2}{I} = 5.07$, $f = 0.67$, $E^* = 3$
p
Δf
$2b^*p$
b^*
.05
.1
.15
1.5
1.3
0.5
1.0
1.1
0.9
0.5
0.9
1.0
1.1
16
12
8
4
0
20
10
0
0.5
1.0
-0.1
0
0.1
-0.67
-0.4
-0.2
0
0.2
0.4
1.0

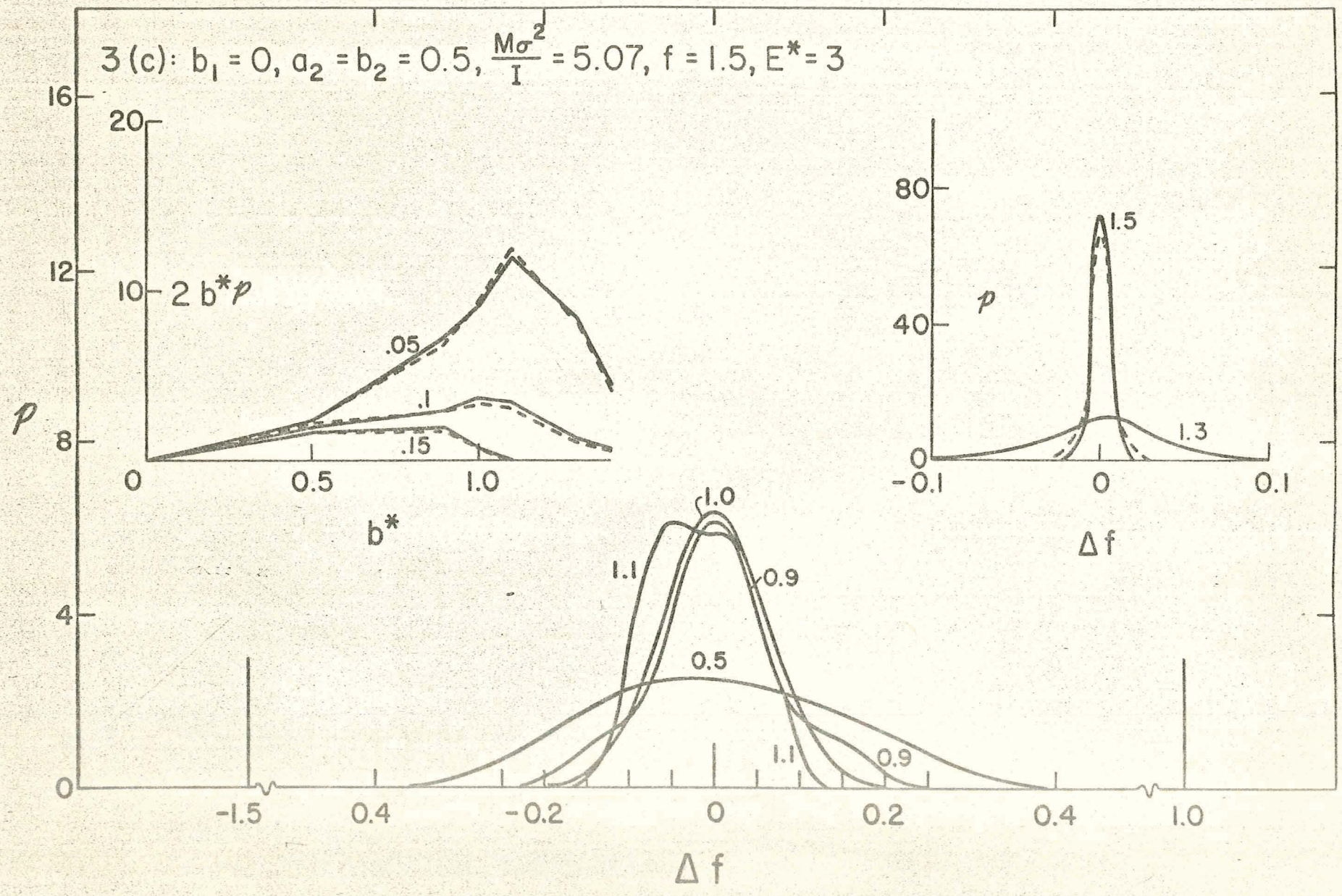
3 (c): $b_1 = 0$, $a_2 = b_2 = 0.5$, $\frac{M\sigma^2}{I} = 5.07$, $f = 1.5$, $E^* = 3$
p
2 b*p
.05
.1
.15
b*
1.5
1.3
Δf
1.0
1.1
0.9
0.5
Δf

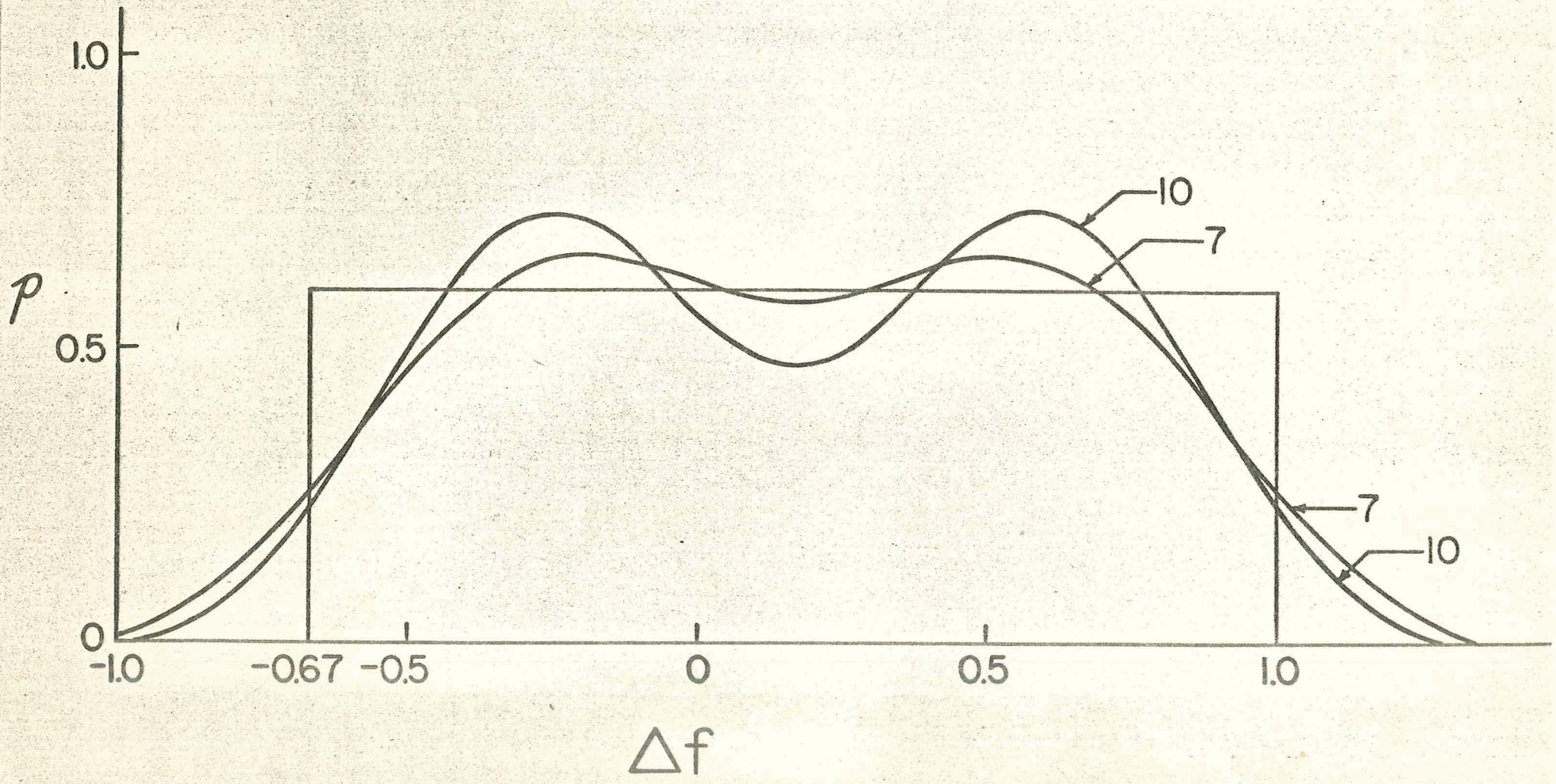

FIGURE 4